Extensional rheology of shear-thickening fumed silica nanoparticles dispersed in an aqueous polyethylene oxide solution

Sunilkumar Khandavalli and Jonathan P. Rothstein[a)]

Mechanical and Industrial Engineering, University of Massachusetts, Amherst, Massachusetts 01003

(Received 3 June 2013; final revision received 15 January 2014; published 19 February 2014)

Synopsis

In this paper, the shear and extensional rheology of fumed silica nanoparticles dispersed in an aqueous polyethylene oxide (PEO) solution is investigated. The role of particle concentration, polymer concentration, and polymer molecular weight on both the shear and the elongational behavior of the dispersions was examined. The fumed silica dispersions were found to strongly shear thicken. Increasing particle concentration was found to increase the degree of shear thickening. The effect of polymer concentration and polymer molecular weight on shear-thickening behavior was found to be nonmonotonic. The data showed a maximum in shear thickening at an optimum polymer concentration and molecular weight. Increasing the polymer concentration and molecular weight was found to reduce the critical shear rate for the onset of shear thickening. Linear viscoelastic measurements showed a qualitatively similar trend in the elastic modulus. Extensional rheology was conducted using a capillary breakup extensional rheometer. The dispersions showed strong strain-hardening behavior with thickening magnitudes similar to that observed under shear. The trends in the magnitude of extensional hardening with particle and polymer concentration were found to be similar to shear. In some cases, extensional thickening of nearly 1000 times was observed. However, in contrast to shear, increasing the molecular weight of the PEO corresponded to a sharp increase in extensional strain-hardening likely due to the role of polymer-induced elasticity which was shown to cause extensional hardening even in the absence of nanoparticles. © *2014 The Society of Rheology*. [http://dx.doi.org/10.1122/1.4864620]

I. INTRODUCTION

Colloidal fluids are ubiquitous in everyday life. These rheologically complex fluids are found in a host of materials ranging from detergents, paints, food, cements, and pharmaceuticals. Due to their current and potential use in myriad applications, colloidal dispersions have been the focus of an enormous amount of interest in both academia [Barnes (1989)] and industry [Wagner and Brady (2009)]. Shear-thickening fluids are one class of colloidal dispersions. In a shear-thickening fluid, the viscosity abruptly increases with increasing shear rate. A classic example is the cornstarch and water mixture known as "oobleck." Shear thickening can often have consequences in fluid handling

[a)]Author to whom correspondence should be addressed; electronic mail: rothstein@ecs.umass.edu

causing damage in industrial processes by breaking equipment or fouling spraying equipment and pumps. Still when properly designed and handled, shear-thickening fluids have been exploited for a wide range of innovative applications. Examples of these applications include developing bullet proof soft body armor [Lee *et al*. (2003)], machine mounts, and damping devices [Helber *et al*. (1990); Laun *et al*. (1991)] and driving fluids for enhanced oil recovery [Nilsson *et al*. (2013)].

The physical mechanism responsible for the shear thickening of colloidal dispersions has been subjected to extensive research and some debate over the last few decades. In the pioneering work of Hoffman (1972, 1974), shear-thickening behavior in concentration latex dispersions was investigated using light scattering of the colloidal fluid. In his measurements, shear thickening was observed to correlate with a loss in Bragg peaks in the scattering patterns. Hoffman (1972) postulated that underlying mechanism was an order-disorder transition in the microstructure at the onset of shear thickening. A decade later, Laun *et al*. (1992) used neutron scattering to show that an order-disorder transition was not required for shear thickening to occur. With the advent of Stokesian dynamics simulations, the onset of shear thickening is now well understood to be the result of the formation of hydroclusters: Dense clusters of tightly packed particles held together by hydrodynamic interactions [Bossis and Brady (1984, 1989)]. Further, experimental studies by researchers [Bender and Wagner (1996); Fagan and Zukoski (1997); Laun *et al*. (1992); Catherall *et al*. (2000); Maranzano and Wagner (2002)] using measurement techniques such as rheology, turbidity, flow small angle neutron scattering, birefringence, and optical dichroism on colloidal dispersions under shear have confirmed the hydrocluster mechanism proposed through Stokesian simulations. Both experiments and simulations have shown that in the regime of shear thickening, where the Peclet number is very large, hydrodynamic lubrication forces dominate all the other colloidal forces resulting in the formation of hydroclusters and an increase in density fluctuations in the fluid. The resulting anisotropy in the colloidal dispersions gives rise to large stress fluctuations and as a result large shear viscosities [Melrose and Ball (2004)].

The shear-thickening behavior strongly depends on several factors such as volume fraction of particles, surface chemistry of the particles, particle size distribution, viscosity of the solvent, and polymer molecular weight [Barnes (1989); Kamibayashi *et al*. (2008)]. However, the dispersions should be stable for shear thickening to occur [Barnes (1989)]. Colloidal dispersions are sterically stabilized by the physical adsorption of free polymer or by chemical grafting polymer chains, onto the surface of colloidal particles. The polymer chains on the surface of colloidal particle prevent the interactions between the particles preventing aggregation or flocculation through steric repulsion [Napper (1983)]. Several researchers have investigated the influence of several factors, such as thickness of polymer grafted layer, polymer molecular weight, particle size, and the viscosity of solvent medium, on the onset of shear-thickening behavior of sterically stabilized colloidal dispersions [Shenoy and Wagner (2005); Frith *et al*. (1996); Mewis and Biebaut (2001); Mewis and Vermant (2000); Kamibayashi *et al*. (2008)]. Raghavan *et al*. (2000) conducted shear and dynamic rheology of fumed silica dispersions in various organic media such as polypropylene glycol (PPG) and polyethylene glycol (PEG) to investigate the influence of various colloidal interactions in the dispersion stability and shear-thickening behavior. Galindo-Rosales and Rubio-Hernandez (2010) and Galindo-Rosales *et al*. (2009) investigated the influence of polymer molecular weight and particle surface chemistry on the shear-thickening behavior by conducting rheology on fumed silica dispersions in PPG. Kamibayashi *et al*. (2008) studied the shear rheology of silica nanoparticles in polyethylene oxide (PEO) and examined the effect of particle concentration, polymer concentration, molecular weight, and particle size on shear-thickening behavior.

The effect of particle concentration was found to increase the magnitude of the shear thickening and decrease the critical shear rate for the onset of shear-thickening behavior. Also, increasing the polymer concentration and polymer molecular weight was found to decrease the critical shear rate needed for the onset of shear-thickening behavior. The shear-thickening behavior was attributed to shear-induced formation of transient network of nanoparticle suspensions flocculated by polymer bridging [Kamibayashi *et al*. (2008)]. The PEO chains have strong affinity of adsorption to the surface of silica nanoparticles through hydrogen bonding [Voronin *et al*. (2004)]. During flow, the shear fields facilitate interaction between polymer chains and particles causing flocculation of the particles by bridging with polymer chains, which result in a shear-thickening behavior [Kamibayashi *et al*. (2008)].

Extensional flows are of significant importance in many applications such as agrochemical spraying, enhanced oil recovery, coating flows, fiber spinning, food processing, and coating flows [Galindo-Rosales *et al*. (2012); Sankaran and Rothstein (2012); Nilsson *et al*. (2013)]. However, there are limited studies dedicated to the extensional rheology of suspensions and colloidal dispersions when compared to shear. Bischoff White *et al*. (2010) studied the extensional rheology of corn starch in water suspensions using filament stretching extensional rheometer (FiSER) and capillary breakup extensional rheometer (CaBER), to investigate the mechanism of strain hardening. The corn starch in water suspensions demonstrated a strong extensional hardening beyond a critical extensional rate. The extensional-hardening behavior was attributed to the aggregation of particle clusters to form interconnected jammed network. Extensional measurements of silica nanoparticles in aqueous polyethylene solution of high molecular weight (4 and 8×10^6 g/mol) using CaBER are presented in the appendix of Wang *et al*. (2004), in connection with the tubeless siphon studies on silica nano suspensions. The nanoparticles in PEO suspensions were found to enhance the extensional flow properties. However, their study was limited to few samples (only two particle concentrations, particle sizes, and PEO molecular weights), and therefore, the trends based on particle concentration, particle size and molecular weight, and the behavioral mechanisms were not investigated systematically. Xu *et al*. (2005) investigated the morphology and rheology of an entangled nanofiber/glycerol-water dispersions using opposed jet device. The dispersions showed extensional thinning behavior which is likely a result of breakdown of entangled nanofiber network structure under extensional stress. Ma *et al*. (2008) used CaBER to investigate the difference in extensional rheology of a Newtonian epoxy and a series of dispersions of carbon nanotubes in the epoxy. The extensional viscosity measurements were in good agreement with theoretical predictions of Batchelor (1971) and Shaqfeh and Fredrickson (1990), who studied rigid rod particles in extensional flows. The extensional viscosity enhancement observed for carbon nanotube dispersions is the result of orientation of carbon nanotube in the flow direction during the stretch. Chellamuthu *et al*. (2009) investigated the extensional rheology of dispersions of fumed silica particles suspended in low molecular weight PPG using filament stretching rheometer combined with light scattering measurements to elucidate the microstructure evolution during the flow. Beyond critical extensional rate, a dramatic increase in strain-hardening of extensional viscosity was observed akin to the thickening transition observed in shear but with a larger magnitude and at reduced critical deformation rates. Light scattering measurements showed that strain-hardening was due to alignment of nanoparticles due to formation of large aggregates in the flow direction. These were the first direct observations of hydrodynamic clustering in extensional flow.

Fumed silica has been an attractive material as a rheological modifier due to its thixotropic behavior and thickening agent. Due to its high specific surface area and branching

structure, it displays remarkable rheological properties. Therefore, fumed silica has tremendous technological applications such as solid electrolytes in fuel cell technology [Lue *et al.* (2010)], stabilizing agent in foams [Binks and Horozov (2005)] and emulsions [Binks (2002)], and viscosity modifier for enhanced oil recovery [Nilsson *et al.* (2013)]. Fumed silica is also widely used as fillers in polymer composites due to improved thermomechanical properties [Nandi *et al.* (2012); Fukushima *et al.* (2011)]. PEO, a water soluble, flexible, nonionic polymer, has potential applications such as lithium ion batters [Lue *et al.* (2010)], turbulent drag reduction [Lim *et al.* (2007)], flocculant in pulp and paper [van de Ven *et al.* (2004)], and drug delivery [Kim *et al.* (2010)]. In the present work, a series of fumed silica colloidal dispersions in a solution of PEO in water were studied. Here, we systematically investigate the effect of particle concentration, polymer concentration, and polymer molecular weight on both shear and extensional behavior.

II. EXPERIMENTAL SETUP

A. Materials

PEO of various molecular weights (2×10^5, 6×10^5, 1×10^6, and 2×10^6 g/mol) was purchased from Aldrich Chemicals. The surface tension of the aqueous PEO solutions in water is ~60 mN/m [Sankaran and Rothstein (2012)]. Hydrophilic fumed silica (AEROSIL @ 200) with specific surface area of 200 m^2/g and primary particle size 12 nm was graciously supplied by Degussa.

B. Sample preparation

Initially PEO solutions were prepared by mixing appropriate amount of PEO in water and stirred for 24 h at room temperature to form homogeneous solution. Fumed silica dispersions were then prepared by adding the appropriate amount of the PEO solution to fumed silica and then sonicated for 20 min. The samples were then stored in air tight glass bottles and were stirred using magnetic stirrer for 12 h before the experiments were performed. The fully mixed dispersions appeared cloudy.

C. Shear rheometry

Shear rheology was conducted on a stress-controlled TA Advantage 2000 and DHR-3 rheometers using a 40 mm aluminum parallel-plate geometry at a constant temperature of 23 °C temperature. A solvent trap was used to prevent sample evaporation during measurements. The samples were pre-sheared before conducting any rheological measurements to erase any shear history during sampling preparation and handing [Raghavan and Khan (1995); Galindo-Rosales and Rubio-Hernandez (2010)]. The pre-shear conditions were determined by observing the evolution of viscosity at different shear rates. The time required to reach a steady-state value at a given shear rate was set as the duration of pre-shear, and the shear rate was chosen below the limit of reversibility to avoid any sample denaturation. Thus, pre-shear conditions were set as pre-shear duration of 4 min at 50 s^{-1} shear rate. After pre-shear, samples were allowed to rest for 4 min to reach equilibrium. Steady shear rheological measurements were conducted in the shear rate range of 0.1–100 s^{-1}, both forward and backward cycles and showed little to no hysteresis. Small amplitude oscillatory shear tests were conducted in the frequency range 0.1 to 100 rad/s, with a fixed strain amplitude, chosen to place the measurements well within the linear viscoelastic region.

D. Capillary breakup extensional rheometry

Extensional measurements were carried out using a CaBER. CaBER is a common technique for characterizing extensional properties of less concentrated and less viscous fluids [McKinley and Tripathi (2000); Anna and McKinley (2001); Rodd *et al*. (2005)]. The CaBER measurements presented here were performed using a high-speed CaBER designed and developed specifically for these experiments. In all of the CaBER experiments presented here, an initial nearly cylindrical fluid sample is placed between two cylindrical plates with radii of $R = 2.5$ mm and stretched with a constant velocity of $U = 200$ mm/s from an initial length $L_i = R$ to final length of L_f. In these experiments, the final stretch length is fixed at $L_f = 3\,L_i$. Once the stretch is stopped, the capillary thinning of the liquid bridge formed between the two end plates or uniaxial extensional flow that is resisted by the viscous and elastic stresses developed by the flow within the filament. A number of rheological properties can be determined by monitoring the evolution of the filaments diameter as a function of time. These include the apparent extensional viscosity, η_E, and the extensional relaxation time, λ_E. The extension rate of the fluid filament is given by

$$\dot{\varepsilon} = -\frac{2}{R_{mid}(t)}\frac{dR_{mid}(t)}{dt}. \tag{1}$$

The evolution of an apparent extensional viscosity with this extension rate profile can easily be calculated by applying a force balance between capillary stresses and the viscous and elastic tensile stresses within the fluid filament neglecting inertia [Anna and McKinley (2001); Papageorgiou (1995)]

$$\eta_{E,app} = \frac{\sigma/R_{mid}(t)}{\dot{\varepsilon}} = \frac{-\sigma}{dD_{mid}(t)/dt}. \tag{2}$$

A number of limiting cases can be theoretically predicted for CaBER measurements. Papageorgiou (1995) showed that for a Newtonian fluid the radius of the fluid filament will decay linearly with time, $R_{mid}(t) \propto (t_b - t)$, to the final breakup at t_b. Entov and Hinch (1997) showed that for an Oldroyd-B fluid with a relaxation time of λ, the radius will decay exponentially with time, $R_{\mathrm{mid}}(t) \propto \exp(-t/3\lambda)$, resulting in a constant extension rate of $\dot{\varepsilon} = 2/3\lambda_E$. However, for particle dispersions, the key is to create a flow strong enough that the Peclet number, $Pe = R^2_{mid}\,\dot{\varepsilon}/D_{12}$, is large and flow dominates the Brownian motion of the particles [Wagner and Brady (2009)]. Here, D_{12} is the diffusion coefficient of the particles in solution.

To calculate the apparent extensional viscosity from experiments, the diameter measurements as a function of time can either be fit with a spline and then differentiated or, for more well-defined fluids such as viscoleastic fluids, the diameter can first be fit with an appropriate functional form and then be differentiated with respect to time [Anna and McKinley (2001)]. For these nanoparticle dispersions, the diameter decay is typically fit with a spline while regions of exponential decay were used to determine the extensional relaxation time of each fluid.

III. RESULTS AND DISCUSSIONS

A. Shear rheology

Prior to investigating shear-thickening behavior of fumed silica dispersions in aqueous PEO, shear rheology was conducted on fumed silica dispersions in water and on neat

PEO solutions separately to examine the rheological behavior independently. The steady shear behavior of the aqueous PEO solutions ($M_w = 6 \times 10^5$ g/mol) appeared Newtonian with a constant viscosity for all concentrations. The viscosity was found to increase approximately linearly with concentration from 2.16 to 14.9 mPa s over the range of PEO concentration tested. Additionally, the linear viscoelastic response of these systems that are not shown here was very weakly elastic and too noisy to obtain reliable, repeatable relaxation time data. Shear rheology of fumed silica dispersions in water at various particle concentrations, without any addition of polymer, is shown in Fig. 1. The pure silica dispersions in water without polymer show shear thinning behavior and do not exhibit any shear thickening. Fumed silica are aggregates synthesized by fusion of spherical SiO_2 with primary particles size of 12 nm into a larger particle that is fractal in nature. Fumed silica nanoparticles in water have been found to exist through small angle neutron scattering as aggregates due to strong hydrogen bonding [Kawaguchi *et al*. (1995)]. The shear thinning behavior could be due to rupture of 3D network of the agglomerates and subsequent orientation of the microstructure along the direction of shear fields [Wagner and Brady (2009); Kawaguchi *et al*. (1996)].

Next, solutions of nanoparticles with PEO were studied in order to understand the impact of particle concentration on shear-thickening behavior. Steady shear experiments were conducted on fumed silica dispersions in aqueous PEO solution where the PEO molecular weight was 6×10^5 g/mol and its concentration was held fixed at 0.6 wt. % but where the fumed silica concentration was varied from 0 to 5 wt. %. As shown in Fig. 2, the dispersions containing PEO showed strong shear-thickening behavior. As expected, the viscosity at low shear rates was observed to increase with increase in particle concentration. At particle concentrations below 3 wt. %, no shear thickening was observed. As the particle concentration was increased, the magnitude in the shear thickening was found to increase monotonically. The degree of shear thickening, η_{max}/η_o, for these samples is also tabulated in Table I. The shear-thickening behavior of fumed silica has been observed in simple solvents like low molecular weight PPG [Raghavan and Khan (1997); Raghavan *et al*. (2000); Chellamuthu *et al*. (2009)]. As described in the Introduction, the mechanism of shear thickening of neat particle dispersions is through the formation of hydroclusters [Bender and Wagner (1996)].

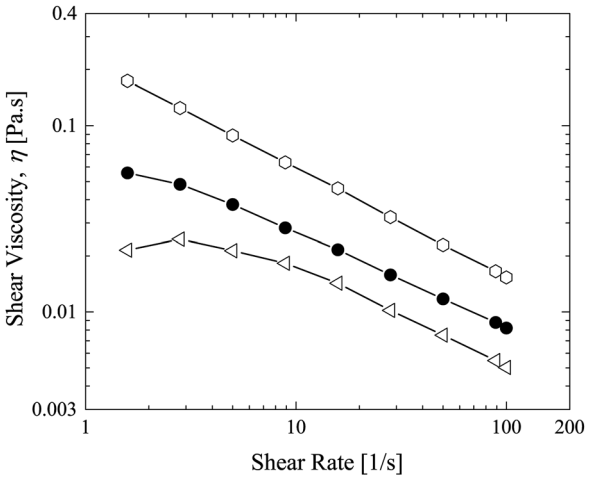

FIG. 1. Steady shear viscosity as a function of shear rate for a series of fumed silica dispersions in water. The data include a series of particle concentrations: (◁) 3 wt. %, (●) 4 wt. %, and (⬡) 5 wt. %.

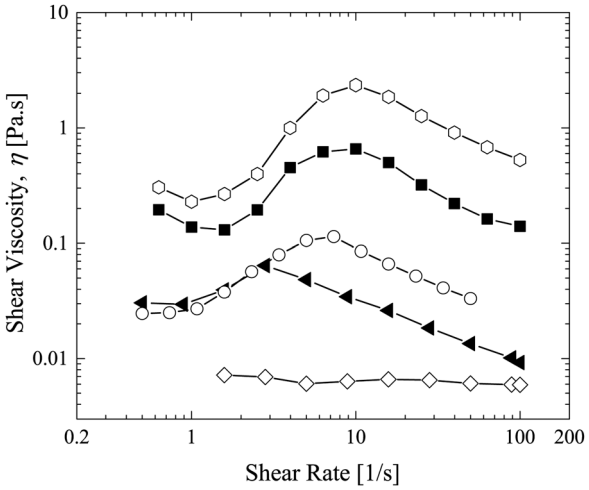

FIG. 2. Steady shear viscosity as a function of shear rate for a series of fumed silica dispersions in 0.6 wt. % PEO ($M_w = 6 \times 10^5$ g/mol). The data include a series of different particle concentrations: (◇) 0 wt. %, (◀) 3 wt. %, (○) 4 wt. %, (■) 4.5 wt. %, and (⬡) 5 wt. %.

PEO has been found to have strong affinity for adsorbing to fumed silica nanoparticles [Voronin *et al*. (2004)]. When PEO is added to the dispersion, they can prevent interaction and control agglomeration of the nanoparticles through the formation of hydrogen bonding between the terminal hydroxyl or the ether group of PEO and the silanol groups of fumed silica. At low shear rates, the particles are influenced only by Brownian motion. Beyond a critical shear rate, the hydrodynamic forces can induce interactions between particles, making it possible for free end of an adsorbed polymer to bridge to another particle creating shear-induced interconnections between particles. Additionally, the adsorbed polymer may be deformed by the imposed shear flow allowing it to extend and bridge with one or more particles creating a 3D interconnected network. The result is likely the formation of particle clusters similar to those formed in the absence of PEO but typically at much lower particle concentrations. This formation of shear-induced clusters of particles flocculated by polymer bridging could result in the shear-thickening behavior [Bender and Wagner (1996); Kamibayashi *et al*. (2008)]. At still higher shear rates, the viscosity is observed to drop as the 3D interconnected network begins to break down under high shear stresses. In Fig. 2, we can observe an increase in the shear-thickening

TABLE I. Rheological properties of fumed silica dispersions in an aqueous PEO.

Sample	M_w (kg/mol)	λ_E (ms)	$Tr = \eta_{E,\infty}/\eta_o$	$\eta_{E,max}/\eta_o$	η_{max}/η_o	$\dot{\gamma}_c$ ($s^{(-1)}$)
3Si-0.6PEO	600	1.4	16.7	1.4	2.2	0.9
4Si-0.6PEO	600	2.2	24.1	1.4	3.7	1.0
4.5Si-0.6PEO	600	3.1	32.0	5.6	4.0	1.5
5Si-0.6PEO	600	6.4	160.0	16.7	9.6	1.0
4.5Si-0.2PEO	600	1.6	10.1	1.8	1.7	10.0
4.5Si-0.4PEO	600	22.4	4000	750	10.0	4.0
4.5Si-0.8PEO	600	1.4	20.0	2.9	1.1	0.6
4.5Si-0.6PEO	200	0.3	31.2	2.5	2.5	8.0
4.5Si-0.6PEO	1000	5.7	38.8	8.2	3.0	1.5
4.5Si-0.6PEO	2000	14.6	70.0	15.9	1.2	0.7

magnitude with increasing particle concentration from 3 to 5 wt. %. Similar trends were observed by Kamibayashi *et al.* (2008). The impact of particle concentration in shear-thickening behavior is also similar to observed for fumed silica dispersions in low molecular weight PPG [Raghavan and Khan (1997); Chellamuthu *et al.* (2009)]. This is likely the result of an increase in the number of silica sites for the PEO chains to adsorb. As a result, the network that is formed at the onset of shear thickening is larger, more interconnected, and stronger. No significant change in the critical shear rate for the onset of shear-thickening behavior can be noticed. However, the maximum in viscosity is observed to shift to larger shear rates indicating a stronger network structure.

Linear viscoelastic measurements were also conducted for different particle concentrations holding PEO concentration constant at 0.6 wt. % as shown in Fig. 3. For all particle concentrations tested, the storage modulus was found to be independent of frequency and significantly larger than the loss modulus, which was found to have a very weak dependency in frequency. This behavior suggests interconnected network of fumed silica nanoparticles dispersions. The increasing trend in the moduli values suggests an increase in the 3D percolation network of fumed silica nanoparticles due to an increase in interparticle and particle-polymer hydrogen bonded interactions.

In order to understand the effect of polymer concentration on shear thickening of these systems, the shear rheology was measured for solutions with varying PEO concentration from 0.2 to 1 wt. % while fixing the fumed silica concentration at 4.5 wt. %. A plot of several representative data sets is shown in Fig. 4. An increase in shear-thickening behavior was observed with increasing PEO concentration up to 0.4 wt. %. At this polymer concentration, the shear-thickening behavior was maximized. Further increases to the PEO concentration resulted in a decrease in shear thickening and eventually, at high PEO concentrations, the elimination of shear thickening. Our hypothesis is that at low polymer concentrations, fewer polymer chains are available to bridge between silica particles. Therefore, the observed increase in shear-thickening behavior with increasing polymer concentration is likely due to increase in the availability of free polymer chains to bridge particles and form hydroclusters. However, increasing the polymer concentration will also simultaneously reduce the number of adsorption sites on the particles available for bridging under flow because they will be occupied or blocked by PEO already adsorbed

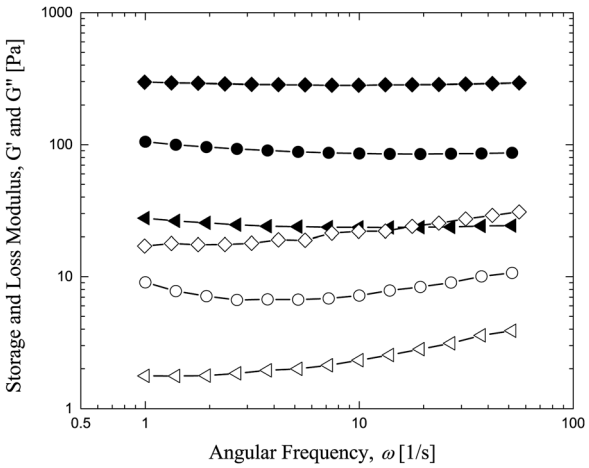

FIG. 3. Storage modulus (filled symbols) and loss modulus (hollow symbols) as a function of angular frequency for a series of fumed silica dispersions in 0.6 wt. % PEO ($M_w = 6 \times 10^5$ g/mol). The data include a series of different particle concentrations: (◀) 3 wt. %, (●) 4 wt. %, and (◆) 5 wt. %.

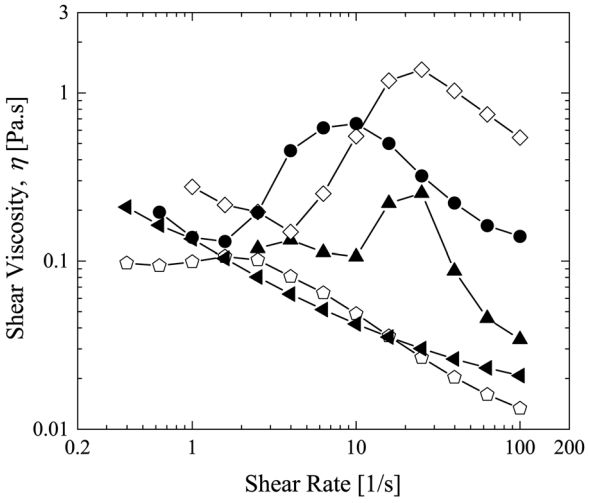

FIG. 4. Steady shear viscosity as a function of shear rate for a series of 4.5 wt. % fumed silica dispersions in an aqueous PEO solution ($M_w = 6 \times 10^5$ g/mol). The data include PEO concentrations of (▲) 0.2 wt. %, (◇) 0.4 wt. %, (●) 0.6 wt. %, (⬠) 0.8 wt. %, and (◀) 1 wt. %.

to the particles under quiescent conditions. Additionally, like polymer brushes attached to a particle [Frith *et al*. (1996)], the adsorbed PEO can increase steric repulsion, increasing the separation between the particles and reducing their hydrodynamic interactions. As a result, a decrease in shear thickening is observed in Fig. 4 beyond a concentration of 0.4 wt. %. Therefore, an optimal polymer concentration exists which maximized the magnitude of shear thickening. Unlike for particle concentrations, a strong correlation can be observed in Fig. 4 between the shear rate required to induce shear thickening and the polymer concentration. Increasing the polymer concentrations from 0.2 to 0.8 wt. % was found to reduce the critical shear rate for the onset of shear thickening by a factor of 10. As flow and Peclet number increase, particle interactions increase as does their proximity due to hydrodynamic interactions [Foss and Brady (2000)]. The critical shear rate for the onset of shear thickening depends on the interparticle distance [Boersma *et al*. (1990)], but also the likelihood of polymer bridging between particles which increases with increasing PEO concentration. The effect of polymer concentration on the onset of shear-thickening behavior observed here is similar to that reported in literature for similar systems [Kamibayashi *et al*. (2008)].

The effect of polymer concentration on linear viscoelastic behavior was also examined and is shown in Fig. 5. The storage modulus exhibits frequency independent behavior in all cases and a nonmonotonic behavior with increasing polymer concentration. The storage modulus initially increases to a maximum and then decreases beyond certain increase in polymer concentration. These measurements and their qualitative similarity to the shear-thickening trends support the physical arguments made above.

In order to understand the effect of molecular weight on the shear behavior, four different polymer molecular weights (2×10^5, 6×10^5, 1×10^6, and 2×10^6 g/mol) were studied. The radius of gyration was estimated using empirical relation of Swenson *et al*. (1998) for PEO solutions in water resulting in values of 28, 53, 72, and 110 nm for 2×10^5, 6×10^5, 1×10^6, and 2×10^6 g/mol molecular weights, respectively. The shear rheology of aqueous solution of 0.6 wt. % PEO without fumed silica particles are also shown in Fig. 6. The behavior is Newtonian up to 1×10^6 g/mol molecular weight and is slightly shear thinning at 2×10^6 g/mol. The viscosity was found to scale linearly with

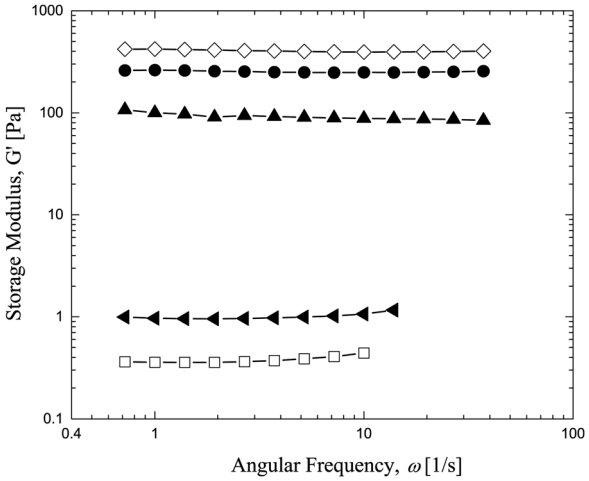

FIG. 5. Storage modulus as a function of frequency for a series of 4.5 wt. % fumed silica dispersions in an aqueous PEO solution ($M_w = 6 \times 10^5$ g/mol). The data include PEO concentrations of (▲) 0.2 wt. %, (◇) 0.4 wt. %, (●) 0.6 wt. %, and (◀) 1 wt. %. The data series for (□) 5 wt. % fumed silica nanoparticle dispersion in water without any polymer is also included.

increasing polymer molecular as expected for dilute polymer solutions [de Gennes (1979)], although a slight deviation from theory at the highest polymer molecular weight was observed. The observed deviation is likely the result of not obtaining a zero shear rate viscosity for the highest molecular weight sample. In Fig. 7, four representative rheological data sets are presented for dispersions of 4.5 wt. % fumed silica nanoparticles in an aqueous solution of 0.6 wt. % PEO. Increasing the molecular weight from 200 to 600 kg/mol increased the shear-thickening behavior. A higher molecular weight polymer has longer chains and can bridge particles farther apart. Additionally, a higher molecular weight polymer can attach to a greater number of particles and increase the degree of bridging [Otsubo (1993)]. As a result, with increase in molecular weight from 2×10^5 to

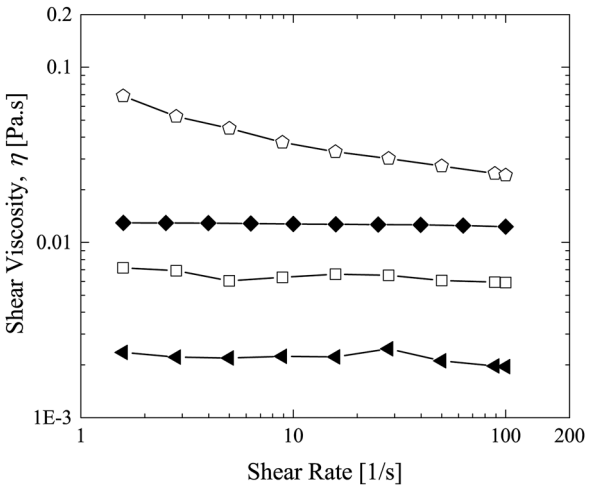

FIG. 6. Steady shear viscosity as a function of shear rate for a series of aqueous 0.6 wt. % PEO solution. The data include a series of PEO at several different molecular weights (M_w): (◀) 2×10^5 g/mol, (□) 6×10^5 g/mol, (◆) 1×10^6 g/mol, and (⬠) 2×10^6 g/mol.

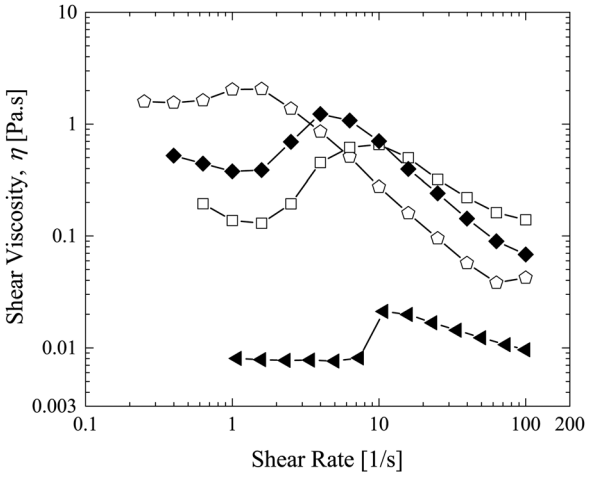

FIG. 7. Steady shear viscosity as a function of shear rate for a series of 4.5 wt. % fumed silica dispersions in an aqueous 0.6 wt. % PEO solution. The data include a series of PEO at several different molecular weights (M_w): (◀) 2×10^5 g/mol, (□) 6×10^5 g/mol, (◆) 1×10^6 g/mol, and (⬠) 2×10^6 g/mol.

6×10^5 g/mol, an increase in the magnitude of shear-thickening behavior was observed. However, increasing the molecular weight further from 6×10^5 to 1×10^6 and finally to 2×10^6 g/mol, the degree of shear thickening, the ratio of peak shear viscosity to the shear viscosity at the onset of thickening, was found to decrease. Here, the comparison between different polymer molecular weights is at a constant weight percent. Therefore, the number of molecules and thus the terminal -OH groups of PEO decrease by a factor of 10 with increasing molecular weight from 2×10^5 to 2×10^6 g/mol. However, the total number of hydrophilic sites of PEO, terminal -OH and ether oxygen groups, remain unchanged as the weight percent is fixed. Therefore, the decrease in the shear-thickening behavior despite constant number of PEO sites suggests a decreasing effectiveness in the formation of bridges between nanoparticles beyond certain increase in the polymer molecular weight. For stable dispersions, the adsorption of a higher molecular weight polymer, whose radius of gyration is greater than the particle, $R_g > R_{particle}$, may result in a significant increase in the polymer coverage of the particle surface area. Kawaguchi *et al.* (2001) have also reported a greater particle surface area coverage at higher polymer molecular weights from the adsorption measurements of PEO onto fumed silica. The observed reduction in shear-thickening could thus be the result of a decreased number of interactions or bridging chains between neighboring nanoparticles [Cabane *et al.* (1997)].

A decrease in the critical shear rate for the onset of shear thickening, $\dot{\gamma}_c$, with increasing molecular weight was also observed. This behavior is consistent with reported in literature [Galindo-Rosales *et al.* (2009); Raghavan *et al.* (2000); Kamibayashi *et al.* (2008)]. Adsorption of a polymer molecule on a particle may also increase the hydrodynamic radius of the particle, which effectively decreases the interparticle distance influencing the onset of shear-thickening behavior. The critical shear rate for shear thickening has been shown to scale inversely with the particle size as $\dot{\gamma}_c \sim a^{-2}$ or a^{-3} [Frith *et al.* (1996); Barnes (1989)].

In order to gain further insights of the effect of polymer molecular weight on shear-thickening, linear viscoelastic experiments were also conducted on the nanoparticle dispersions at different polymer molecular weights as shown in Fig. 8. At 2×10^5 and 6×10^5 g/mol PEO molecular weight, the moduli variation is frequency independent indicating an interconnected structure. However, increasing the molecular weight to

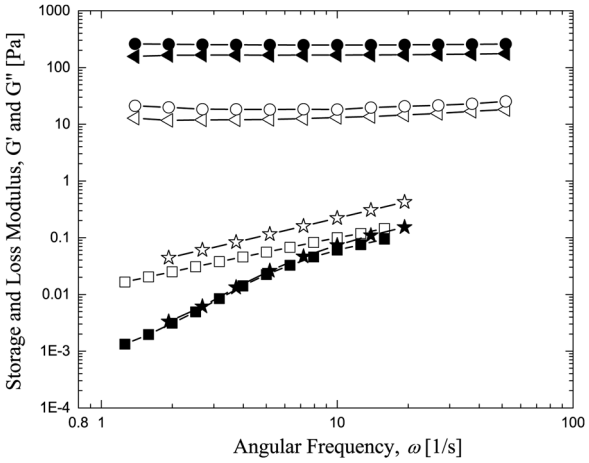

FIG. 8. Storage modulus (filled symbols) and loss modulus (hollow symbols) as a function of angular frequency for a series of 4.5 wt. % fumed silica nanoparticle dispersions in an aqueous 0.6 wt. % PEO solution. The data include a series of PEO at several different molecular weights (M_w): (◀) 2×10^5 g/mol, (●) 6×10^5 g/mol, and (■) 2×10^6 g/mol. The data (⋆) for 0.6 wt. % aqueous PEO of molecular weight 2×10^6 g/mol without fumed silica nanoparticles are also included.

2×10^6 g/mol results in a sol-like response ($G'' > G'$) with moduli scaling power law with frequency, approaching $G' \sim \omega^2$ and $G'' \sim \omega$ at low frequency. Further, the frequency sweep response is quite similar to the case with pure polymer solution without any nanoparticles. This suggests that for the high molecular weight systems, the polymer and not the particles dominate the fluid's response. These results agree well with Kawaguchi *et al*. (2001) who reported a similar reduction in the dynamic moduli for adsorption of higher PEO molecular weight to silica nanoparticles.

B. Extensional rheology

Capillary breakup extensional rheology of the silica dispersions was conducted varying particle concentration, polymer concentration, and molecular weight as described in Sec. II D. In Fig. 9, the evolution of the diameter for a series of silica particle concentrations is shown on a semi-log plot. Here, the concentration and molecular weight of PEO are fixed at 0.6 wt. % and 6×10^5 g/mol, respectively. We can observe an increase in filament lifetime with increasing particle concentration. In order to calculate the apparent extensional viscosity, the diameter decay data were fit by a spline and then differentiated according to Eq. (2). In Fig. 10, the apparent extensional viscosity, η_E, is shown as a function of Hencky strain for various particle concentrations. The apparent extensional viscosity is independent of Hencky strain at low strains, begins to increase beyond a certain Hencky strain, and levels off at high Hencky strains. This behavior is termed as strain hardening. As expected, the apparent extensional viscosity at low strains, $\eta_{E,o}$, increases with increase in particle concentration. The Trouton ratio, $Tr = \eta_{E,o}/\eta_o$, was found to be in the range of 5–10, which is slightly larger than 3, which is predicted for Newtonian fluids. There is some uncertainty as to which zero shear rate viscosity to choose as many of these samples show shear thinning even at the lowest shear rates measured. The value for η_o is thus likely a little low for all these samples. Additionally, the particles are not spherical, and Batchelor (1971) showed that high aspect ratio particles can have large extensional viscosities. Thus, the deviation from $Tr = 3$ could be due to the nonspherical or fractal nature of the fumed silica particles [Batchelor (1971)]. The strain-hardening

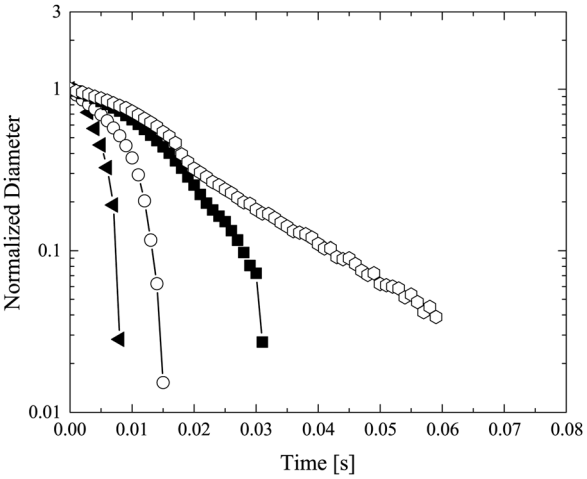

FIG. 9. Diameter evolution as a function of time during a capillary breakup extensional rheology measurement for a series of fumed silica dispersions in an aqueous solution of 0.6 wt. % PEO ($M_w = 6 \times 10^5$ g/mol). The data include a number of different particle concentrations: (◀) 3 wt. %, (○) 4 wt. %, (■) 4.5 wt. %, and (⬡) 5 wt. %.

behavior is mild at lower particle concentrations but increases strongly at higher particle concentration. The steady-state Trouton ratio, $Tr_\infty = \eta_{E,\infty}/\eta_o$, and extensional relaxation time as a function of particle concentration are shown in Fig. 11. The extensional relaxation time, λ_E, was obtained by fitting the exponential diameter decay in the middle times to an exponential function. The characteristic extensional relaxation times thus calculated for various particle concentrations are shown in Fig. 11. We can observe an increase in λ_E with increase in particle concentration. We notice that the Tr_∞ and λ_E increase quite quickly with increase in particle concentration beyond a 4 wt. % particle concentration to a maximum of $Tr_\infty = 160$ and $\lambda_E = 6.4$ ms, respectively. The qualitative effect of particle concentration on strain hardening is consistent with the observations in literature [Wang *et al*. (2004); Chellamuthu *et al*. (2009)]. In Chellamuthu *et al*. (2009), the light scattering

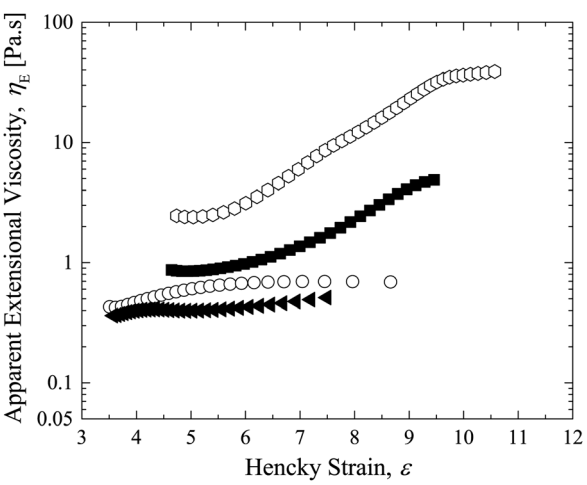

FIG. 10. Apparent extensional viscosity as a function of Hencky strain for a series of fumed silica dispersions in an aqueous 0.6 wt. % PEO solution (M_w: 6×10^5 g/mol). The data include several different particle concentrations: (◀) 3 wt. %, (○) 4 wt. %, (■) 4.5 wt. %, and (⬡) 5 wt. %.

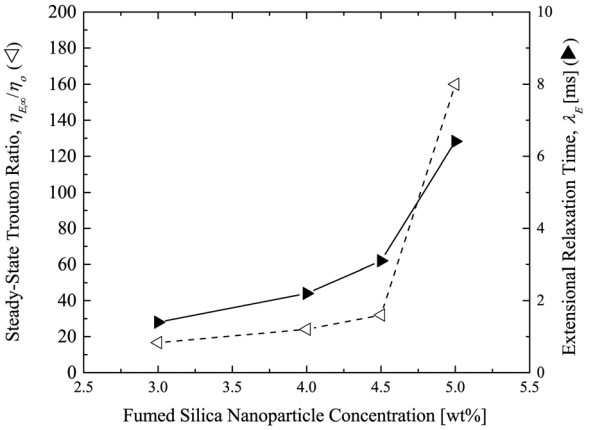

FIG. 11. Steady-state Trouton ratio $\eta_{E,\infty}/\eta_o$ (◁) and extensional relaxation time λ_E (▶) as a function of fumed silica nanoparticle concentration in 0.6 wt. % aqueous PEO solution ($M_w = 6 \times 10^5$ g/mol).

measurements during the extensional flow of fumed silica dispersions in low molecular weight PPG indicated an alignment of string of interacting particles in the flow direction. We believe alignment and interaction of particles in the extensional flows presented here can result in the formation of multiple particle clusters bridged by the PEO chains, resulting in the strong strain-hardening behavior presented in Fig. 10. The increase in the strain-hardening behavior with increasing silica particle concentration could be the result of increased bridging between particles and polymer chains and the development of a stronger interparticle network structure as was observed in the shear rheology and linear viscoelastic measurements.

In shear rheology, a strong correlation between elastic modulus and shear-thickening behavior by polymer-particle bridging mechanism has been demonstrated. Here, we examine the trends in the elongational behavior as compared to shear-thickening to understand the mechanism of strain-hardening in elongational flow. The effect of particle concentration in the trends of shear-thickening and strain-hardening is compared in Fig. 12. The magnitude of strain hardening was quantified as the ratio of steady-state apparent extensional viscosity and the apparent extensional viscosity at low Hencky strains, $\eta_{E,o}$.

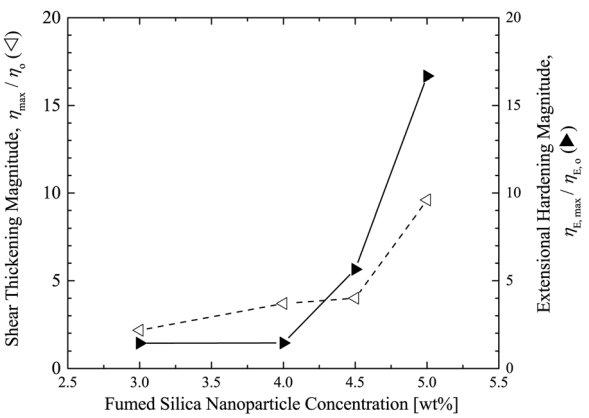

FIG. 12. Shear-thickening magnitude η_{max}/η_o (◁) and extensional-hardening magnitude $\eta_{E,max}/\eta_o$ (▶) as a function of fumed silica nanoparticle concentration in 0.6 wt. % aqueous PEO solution ($M_w = 6 \times 10^5$ g/mol).

Similarly, the magnitude of shear thickening was calculated as the ratio of the maximum attained viscosity in the shear-thickening range and the viscosity at the onset of shear thickening, η_{max}/η_c. We can observe that both the magnitude of shear and extensional thickening show an increasing trend with increasing particle concentration. The effect of particle concentration on strain-hardening behavior is qualitatively similar to the shear-thickening behavior. This suggests a similarity in the mechanism of strain-hardening and shear-thickening behavior. However, the increase in the extensional-hardening magnitude is greater than the shear-thickening magnitude at higher particle concentrations. Finally, we should note that the extensional rheology of pure fumed silica dispersions was not possible to measure because, due to the low viscosity of the samples, the filament breakup time scales are too fast to accurately capture the capillary thinning process.

In order to understand the effect of polymer concentration on extensional rheology, CaBER measurements were conducted on a series of samples with varying polymer concentration from 0.2 to 0.8 wt. % with a particle concentration fixed at 4.5 wt. % and a polymer molecular weight of 6×10^5 g/mol. The results are presented in Fig. 13. As with shear, we observed a nonmonotonic trend in the magnitude of strain hardening with increasing PEO concentration. The strain-hardening behavior increases up to 0.4 wt. % PEO and then decreases with further increase in PEO concentration. At 0.4 wt. % PEO, the steady-state apparent extensional viscosity was found to increase by three orders of magnitude and continued increasing to very high Hencky strains. The steady-state Trouton ratio and extensional relaxation time are shown as a function of PEO concentration in Fig. 14. A maximum in both the steady-state Trouton ratio and the extensional relaxation time are observed at a PEO concentration of 0.4 wt. % suggesting a clear optimal PEO concentration for both the shear and extensional thickening in these systems. The effect of PEO concentration on strain hardening and shear thickening is compared in Fig. 15. We can observe that the trends in the magnitude of strain-hardening and shear-thickening behavior with increasing PEO concentration are qualitatively similar, where a maximum in both the behavior occurs at an optimum PEO concentration, which also occurs at the same 0.4 wt. % PEO concentration. This strongly suggests that the effect of PEO concentration in strain-hardening mechanism is similar to shear thickening.

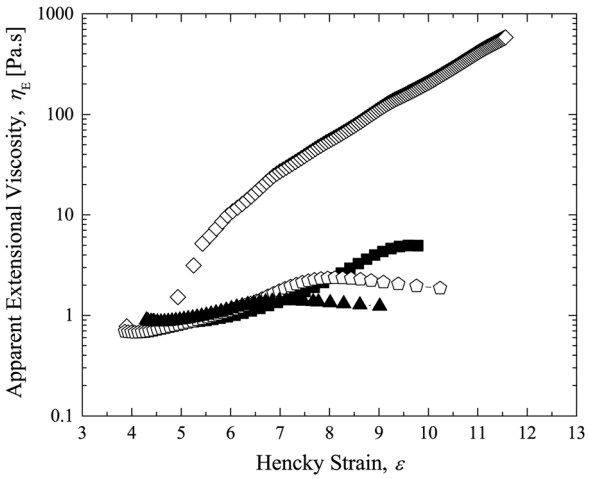

FIG. 13. Apparent extensional viscosity as a function of Hencky strain for a series of 4.5 wt. % fumed silica nanoparticle dispersions ($M_w = 6 \times 10^5$ g/mol) in water. The data include results for a number of different PEO concentrations: (▲) 0.2 wt. %, (◇) 0.4 wt. %, (■) 0.6 wt. %, and (⬠) 0.8 wt. %.

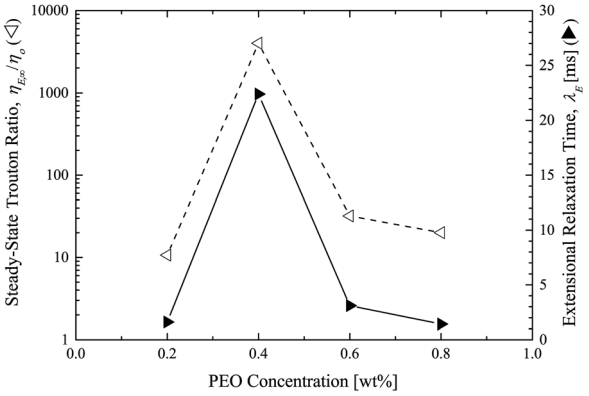

FIG. 14. Steady-state Trouton ratio $\eta_{E,\infty}/\eta_o$ (◁) and extensional relaxation time λ_E (▶) as a function of PEO concentration ($M_w = 6 \times 10^5$ g/mol) at 4.5 wt. % fumed silica concentration.

However, the increase in the extensional-hardening magnitude is approximately two orders of magnitude greater than the shear-thickening magnitude.

In order to understand the effect of polymer molecular weight, extensional rheology measurements of fumed silica nanoparticle dispersions in aqueous PEO solution were performed for a series of solutions using four different molecular weights of PEO, 2×10^5, 6×10^5, 1×10^6, and 2×10^6 g/mol as shown in Fig. 16. Here, the fumed silica concentration and PEO concentration are fixed at 4.5 and 0.6 wt. %, respectively. As expected, the apparent extensional viscosity at low Hencky strains was found to equal approximately $Tr \sim 3$ and increase with increasing molecular weight. At large Hencky strains, the magnitude of strain hardening was found to also increase with increasing polymer molecular weight. As seen in Fig. 17, these trends correspond to an increase in extensional relaxation time and steady-state Trouton ratio with increase in molecular weight. The effect of polymer molecular weight on the strain-hardening behavior is in agreement with reported for silica nanoparticle suspensions in high molecular weight PEO (4 and 8×10^6 g/mol) [Wang *et al.* (2004)]. Extensional rheology measurements for 2×10^6 g/mol molecular weight without any nanoparticles is also shown in Fig. 16. The apparent extensional viscosity at low Hencky strains is lower compared to the dispersions of nanoparticles as expected. However, the magnitude of strain-hardening was found to

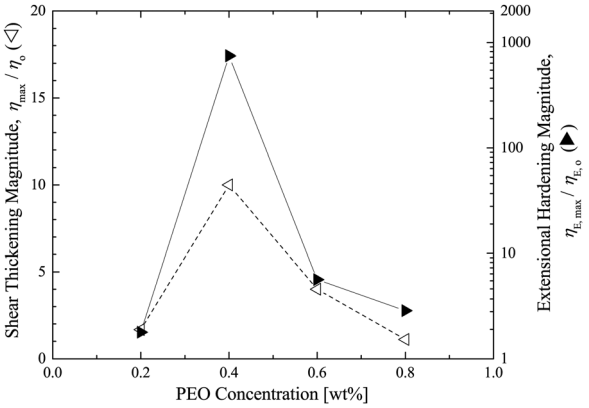

FIG. 15. Shear-thickening magnitude η_{max}/η_o (◁) and extensional-hardening magnitude $\eta_{E,max}/\eta_o$ (▶) as a function of PEO concentration ($M_w = 6 \times 10^5$ g/mol) for a 4.5 wt. % fumed silica nanoparticle concentration.

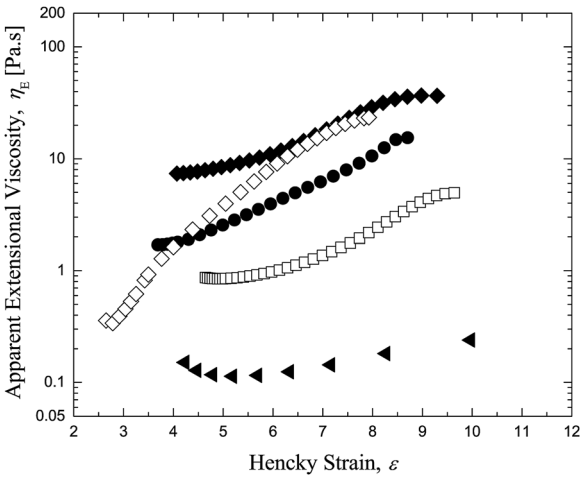

FIG. 16. Apparent extensional viscosity as a function of Hencky strain for a series of 4.5 wt. % fumed silica nanoparticle dispersions in an aqueous 0.6 wt. % PEO solutions in water. The data include results for a number of different PEO molecular weights: (◀) 2×10^5, (□) 6×10^5, (●) 1×10^6 g/mol, and (◆) 2×10^6 g/mol. The data (◇) for 0.6 wt. % aqueous PEO of molecular weight 2×10^6 g/mol without fumed silica nanoparticles are also included.

be about two times greater than the dispersions containing nanoparticles. The elongational measurements for the PEO solutions of molecular weight lower than 2×10^6 g/mol could not be measured due to their low viscosity and the resulting extremely short life times of their filaments.

If we compare the effect of polymer molecular weight in both shear and extensional rheology by observing the trends of the magnitude of shear-thickening and extensional hardening with increasing molecular weight in Fig. 18, we notice qualitatively different trends in the behavior. The shear-thickening trend is nonmonotonic with increasing molecular weight, where a maximum in shear-thickening behavior occurs at $M_w = 6 \times 10^5$ g/mol. Conversely, the strain-hardening behavior was found to increase monotonically with increase in the molecular weight. The contrasting trends between

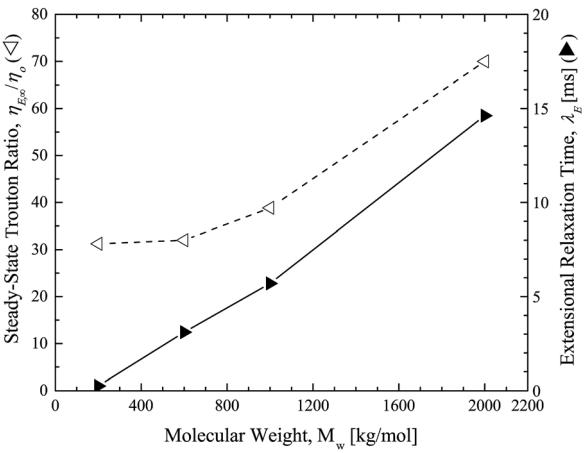

FIG. 17. Steady-state Trouton ratio $\eta_{E,\infty}/\eta_o$ (◁) and extensional relaxation time λ_E (▶) as a function of PEO molecular weight. The concentration of aqueous PEO and fumed silica nanoparticles is at 0.6 wt. % and 4.5 wt. %, respectively.

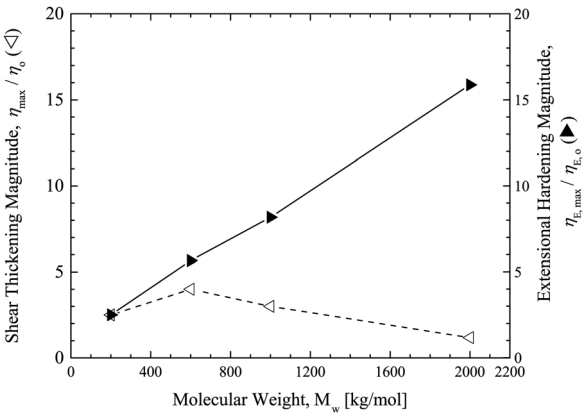

FIG. 18. Shear-thickening magnitude η_{max}/η_o (◁) and extensional-hardening magnitude $\eta_{E,max}/\eta_o$ (▶) as a function of PEO molecular weight. The concentration of aqueous PEO and fumed silica nanoparticles is at 0.6 wt. % and 4.5 wt. % respectively.

shear-thickening and strain-hardening behavior suggest that the polymer chain length plays a different role in shear versus extensional flows. Clearly polymer elasticity and the deformation of polymer chains either in bulk or tethered between nanoparticles have a significant impact in the strain-hardening mechanism for these nanoparticle/high molecular weight dispersions.

IV. CONCLUSIONS

The effect of particle concentration, polymer concentration, and polymer molecular weight on both shear and elongational behaviors of fumed silica dispersions was investigated. In shear, increasing particle concentration was found to increase the extent of shear thickening. The effect of polymer concentration and molecular weight on the shear-thickening behavior was qualitatively similar. In each cases, a maximum shear thickening was found to occur at either an optimum polymer concentration or polymer molecular weight. In addition, increasing the polymer concentration and the polymer molecular weight was found to decrease the critical shear rate for the onset of shear thickening. The shear-thickening behavior was attributed to the formation of hydroclusters resulting from the polymer-particle bridging induced by the imposed shear flows. Linear viscoelastic measurements showed strong correlation between the trends in the elastic modulus and the shear-thickening behavior. Extensional rheological measurements were conducted using CaBER. The effect of particle concentration and polymer concentration on the strain-hardening behavior was found to be qualitatively similar to shear thickening. The similarity in the fluids response under shear and extension indicated a similar underlying physical mechanism. Increasing the particle concentration increased the magnitude of strain hardening similar to shear thickening. However, the increase in the magnitude of strain hardening is larger compared to the shear thickening at higher particle concentrations. With increasing polymer concentration, the strain-hardening behavior showed a nonmonotonic trend similar to shear thickening. At optimal conditions of 0.4 wt. % PEO concentration, 6×10^6 g/mol molecular weight, and 4.5 wt. % fumed silica nanoparticle concentration, an enormous increase in the extensional viscosity was observed. Though the maximum in both the shear-thickening and strain-hardening behaviors occurred at the same optimal conditions, the magnitude of strain hardening was found to be

approximately two orders of magnitude larger than the shear thickening. The extensional strain-hardening mechanism is likely due to the polymer-particle bridging induced by flow. The study of the effect of polymer molecular weight on strain-hardening behavior showed a contrasting trend to shear-thickening behavior. The strain-hardening behavior increased monotonically with increasing polymer molecular weight, as opposed to a maximum shear thickening at an optimum polymer molecular weight. This indicates the significant role of polymer elasticity in the elongational behavior at higher polymer molecular weight that predominates the hydrocluster mechanism in the shear-thickening behavior.

ACKNOWLEDGMENT

The authors would like to thank National Science of Foundation for funding the current project through the Center for Hierarchical Manufacturing at UMASS under Grant No. CMMI-1025020.

References

Anna, S. L., and G. H. McKinley, "Elasto-capillary thinning and breakup of model elastic liquids," J. Rheol. **45**, 115–138 (2001).

Barnes, H., "Shear-thickening (dilatancy) in suspensions of nonaggregating solid particles dispersed in Newtonian liquids," J. Rheol. **33**, 329–366 (1989).

Batchelor, G., "The stress generated in a non-dilute suspension of elongated particles by pure straining motion," J. Fluid Mech. **46**, 813–829 (1971).

Bender, J., and N. J. Wagner, "Reversible shear thickening in monodisperse and bidisperse colloidal dispersions," J. Rheol. **40**, 899–916 (1996).

Binks, B. P., "Particles as surfactants similarities and differences," Curr. Opin. Colloid Interface Sci. **7**, 21–41 (2002).

Binks, B. P., and T. S. Horozov, "Aqueous foams stabilized solely by silica nanoparticles," Angew. Chem. **117**, 3788–3791 (2005).

Bischoff White, E. E., M. Chellamuthu, and J. P. Rothstein, "Extensional rheology of a shear-thickening cornstarch and water suspension," Rheol. Acta **49**, 119–129 (2010).

Boersma, W. H., J. Laven, and H. N. Stein, "Shear thickening (dilatancy) in concentrated dispersions," AIChE J. **36**, 321–332 (1990).

Bossis, G., and J. F. Brady, "Dynamic simulation of sheared suspensions. 1. General method," J. Chem. Phys. **80**, 5141–5154 (1984).

Bossis, G., and J. F. Brady, "The rheology of Brownian suspensions," J. Chem. Phys. **91**, 1866–1874 (1989).

Cabane, B., K. Wong, P. Lindner, and F. Lafuma, "Shear induced gelation of colloidal dispersions," J. Rheol. **41**, 531–547 (1997).

Catherall, A. A., J. R. Melrose, and R. C. Ball, "Shear thickening and order-disorder effects in concentrated colloids at high shear rates," J. Rheol. **44**, 1–25 (2000).

Chellamuthu, M., E. Arndt, and J. P. Rothstein, "Extensional rheology of shear-thickening nanoparticle suspensions," Soft Matter **5**, 2117–2124 (2009).

de Gennes, P.-G., *Scaling Concepts in Polymer Physics* (Cornell University Press, New York, 1979).

Entov, V., and E. Hinch, "Effect of a spectrum of relaxation times on the capillary thinning of a filament of elastic liquid," J. Non-Newtonian Fluid Mech. **72**, 31–53 (1997).

Fagan, M. E., and C. F. Zukoski, "The rheology of charge stabilized silica suspensions," J. Rheol. **41**, 373–397 (1997).

Foss, D. R., and J. F. Brady, "Structure, diffusion and rheology of Brownian suspensions by Stokesian Dynamics simulation," J. Fluid Mech. **407**, 167–200 (2000).

Frith, W. J., P. d'Haene, R. Buscall, and J. Mewis, "Shear thickening in model suspensions of sterically stabilized particles," J. Rheol. **40**, 531–548 (1996).

Fukushima, K., D. Tabuani, C. Abbate, M. Arena, and P. Rizzarelli, "Preparation, characterization and biodegradation of biopolymer nanocomposites based on fumed silica," Eur. Polym. J. **47**, 139–152 (2011).

Galindo-Rosales, F. J., and F. J. Rubio-Hernandez, "Static and dynamic yield stresses of Aerosil @ 200 suspension in polypropylene glycol," Appl. Rheol. **20**, 22787 (2010).

Galindo-Rosales, F. J., F. J. Rubio-Hernandez, and J. F. Vel'azquez-Navarro, "Shear- thickening behavior of Aerosil @ R816 nanoparticles suspensions in polar organic liquids," Rheol. Acta **48**, 699–708 (2009).

Galindo-Rosales, F. J., M. Alves, and M. Oliveira, "Microdevices for extensional rheometry of low viscosity elastic liquids: A review," Microfluid. Nanofluid. **14**, 1–19 (2013).

Helber, R., F. Doncker, and R. Bung, "Vibration attenuation by passive stiffness switching mounts," J. Sound Vib. **138**, 47–57 (1990).

Hoffman, R. L., "Discontinuous and dilatant viscosity behavior in concentrated suspensions. I. Observation of a flow instability," J. Rheol. **16**, 155–173 (1972).

Hoffman, R. L., "Discontinuous and dilatant viscosity behavior in concentrated suspensions. II. Theory and experimental tests," J. Colloid Interface Sci. **46**, 491–506 (1974).

Kamibayashi, M., H. Ogura, and Y. Otsubo, "Shear-thickening flow of nanoparticle suspensions flocculated by polymer bridging," J. Colloid Interface Sci. **321**, 294–301 (2008).

Kawaguchi, M., T. Yamamoto, and T. Kato, "Rheological studies of hydrophilic and hydrophobic silica suspensions in the presence of adsorbed poly(N-isopropylacrylamide)," Langmuir **12**, 6184–6187 (1996).

Kawaguchi, M., T. Yamamoto, and T. Kato, "Rheological properties of silica suspensions in aqueous solutions of block copolymers and their water-soluble components," J. Colloid Interface Sci. **241**, 293–295 (2001).

Kawaguchi, M., Y. Kimura, T. Tanahashi, J. Takeoka, J.-I. Suzuki, T. Kato, and S. Funahashi, "Polymer adsorption effects on structures and rheological properties of silica suspensions," Langmuir **11**, 563–567 (1995).

Kim, G., H. Yoon, and Y. Park, "Drug release from various thicknesses of layered mats consisting of electrospun polycaprolactone and polyethylene oxide micro/nanofibers," Appl. Phys. A **100**, 1197–1204 (2010).

Laun, H. M., R. Bung, and F. Schmidt, "Rheology of extremely shear thickening polymer dispersions (passively viscosity switching fluids)," J. Rheol. **35**, 999–1034 (1991).

Laun, H. M., R. Bung, S. Hess, W. Loose, O. Hess, K. Hahn, E. Hadicke, R. Hingmann, F. Schmidt, and P. Lindner, "Rheological and small-angle neutron-scattering investigation of shear-induced particle structures of concentrated polymer dispersions submitted to plane Poiseuille and Couette-flow," J. Rheol. **36**, 743–787 (1992).

Lee, Y., E. Wetzel, and N. Wagner, "The ballistic impact characteristics of Kevlar woven fabrics impregnated with a colloidal shear thickening fluid," J. Mater. Sci. **38**, 2825–2833 (2003).

Lim, S. T., C. H. Hong, H. J. Choi, P.-Y. Lai, and C. K. Chan, "Polymer turbulent drag reduction near the theta point," Europhys. Lett. **80**, 58003 (2007).

Lue, S. J., W.-T. Wang, K. Mahesh, and C. C. Yang, "Enhanced performance of a direct methanol alkaline fuel cell (DMAFC) using a polyvinyl alcohol/fumed silica/KOH electrolyte," J. Power Sources **195**, 7991–7999 (2010).

Ma, A. W. K., F. Chinesta, T. Tuladhar, and M. R. Mackley, "Filament stretching of carbon nanotube suspensions," Rheol. Acta **47**, 447–457 (2008).

Maranzano, R., and N. J. Wagner, "Flow-small angle neutron scattering measurements of colloidal dispersion microstructure evolution through the shear thickening transition," J. Chem. Phys. **117**, 10291–10302 (2002).

McKinley, G. H., and A. Tripathi, "How to extract the Newtonian viscosity from capillary breakup measurements in a filament rheometer," J. Rheol. **44**, 653–670 (2000).

Melrose, J. R., and R. C. Ball, "Continuous shear thickening transitions in model concentrated colloids—The role of interparticle forces," J. Rheol. **48**, 937–960 (2004).

Mewis, J., and G. Biebaut, "Shear thickening in steady and superposition flows effect of particle interaction forces," J. Rheol. **45**, 799–813 (2001).

Mewis, J., and J. Vermant, "Rheology of sterically stabilized dispersions and lattices," Prog. Org. Coat. **40**, 111–117 (2000).

Nandi, S., S. Bose, S. Mitra, and A. K. Ghosh, "Dynamic rheology and morphology of HDPE-fumed silica composites: Effect of interface modification," Polym. Eng. Sci. **53**, 644–650 (2013).

Napper, D., *Polymeric Stabilization of Colloidal Dispersions* (Academic, New York, 1983).

Nilsson, M. A., R. Kulkarni, L. Gerberich, R. Hammond, R. Singh, and J. P. Rothstein, "The effect of fluid rheology on enhanced oil recovery using a microfluidic sandstone device," J. Non-Newtonian Fluid Mech. **202**, 112–119 (2013).

Otsubo, Y., "Size effects on the shear-thickening behavior of suspensions flocculated by polymer bridging," J. Rheol. **37**, 799–809 (1993).

Papageorgiou, D., "On the breakup of viscous liquid threads," Phys. Fluids **7**, 1529–1544 (1995).

Raghavan, S. R., H. J. Walls, and S. A. Khan, "Rheology of silica dispersions in organic liquids: New evidence for solvation forces dictated by hydrogen bonding," Langmuir **16**, 7920–7930 (2000).

Raghavan, S. R., and S. Khan, "Shear-thickening response of fumed silica suspensions under steady and oscillatory shear," J. Colloid Interface Sci. **185**, 57–67 (1997).

Raghavan, S. R., and S. A. Khan, "Shear-induced microstructural changes in flocculated suspensions of fumed silica," J. Rheol. **39**, 1311–1325 (1995).

Rodd, L. E., T. Scott, J. Cooper-White, and G. McKinley, "Capillary break-up rheometry of low-viscosity elastic fluids," Appl. Rheol. **15**, 12–27 (2005).

Sankaran, A. K., and J. P. Rothstein, "Effect of viscoelasticity on liquid transfer during gravure printing," J. Non-Newtonian Fluid Mech. **175–176**, 64–75 (2012).

Shaqfeh, E. S. G., and G. H. Fredrickson, "The hydrodynamic stress in a suspension of rods," Phys. Fluids A **2**, 7–24 (1990).

Shenoy, S., and N. Wagner, "Influence of medium viscosity and adsorbed polymer on the reversible shear thickening transition in concentrated colloidal dispersions," Rheol. Acta **44**, 360–371 (2005).

Swenson, J., M. V. Smalley, and H. L. M. Hatharasinghe, "Mechanism and strength of polymer bridging flocculation," Phys. Rev. Lett. **81**, 5840–5843 (1998).

van de Ven, T. G. M., M. A. Qasaimeh, and J. Paris, "PEO-induced flocculation of fines: Effects of PEO dissolution conditions and shear history," Colloids Surf., A **248**, 151–156 (2004).

Voronin, E., V. Gun'ko, N. Guzenko, E. Pakhlov, L. Nosach, R. Leboda, J. Skubiszewska-Ziba, M. Malysheva, M. Borysenko, and A. Chuiko, "Interaction of poly(ethylene oxide) with fumed silica," J. Colloid Interface Sci. **279**, 326–340 (2004).

Wagner, N. J., and J. F. Brady, "Shear thickening in colloidal dispersions," Physics Today **62**(10), 27–32 (2009).

Wang, J., R. Bai, and D. D. Joseph, "Nanoparticle-laden tubeless and open siphons," J. Fluid Mech. **516**, 335–348 (2004).

Xu, J., S. Chatterjee, K. W. Koelling, Y. Wang, and S. E. Bechtel, "Shear and extensional rheology of carbon nanofiber suspensions," Rheol. Acta **44**, 537–562 (2005).